Supramolecular Chirogenesis in Zinc Porphyrins: Mechanism, Role of Guest Structure, and Application for the Absolute Configuration Determination

Victor V. Borovkov,* Juha M. Lintuluoto, and Yoshihisa Inoue*

Contribution from the Inoue Photochirogenesis Project, ERATO, JST, 4-6-3 Kamishinden, Toyonaka-shi, Osaka 560-0085, Japan

Received September 7, 2000

Abstract: The achiral *syn* folded (face-to-face conformation) host molecule of the ethane-bridged bis(zinc porphyrin) transforms into the corresponding chiral extended *anti* bis-ligated species in the presence of enantiopure amine guests. The mechanism of the supramolecular chirogenesis is based upon the screw formation in bis(zinc porphyrin), arising from steric interactions between the largest substituent at the ligand's asymmetric carbon and peripheral alkyl groups of the neighboring porphyrin ring pointing toward the covalent bridge. The screw direction is determined by the guest's (amines) absolute configuration resulting in a positive chirality induced by (*S*)-enantiomers due to formation of the right-handed screw, and a negative chirality produced by the left-handed screw of (*R*)-enantiomers. The screw magnitude is strongly dependent upon the structure of the chiral guests. The amines with bulkier substituents result in stronger CD signals and larger ^{1}H NMR resonance splittings of enantiotopic protons. This system possesses a high degree of chiroptical activity, which allows the differentiation of one of the smallest homologous elements of organic chemistry, that is, the methyl and ethyl groups attached to the asymmetric carbon, and additionally, which senses a remote chiral center at a position β to the amine binding group.

Introduction

Supramolecular chirality is a relatively new area of interdisciplinary research in modern chemical sciences, which combines supramolecular chemistry and molecular chirality. This branch of chemistry deals with the asymmetry phenomenon in molecular assemblies linked via noncovalent interactions. Two of the most scientifically interesting and practically important directions in this field are "symmetry breaking" in intrinsically achiral multi- or unimolecular systems and chirality amplification in supramolecular assemblies consisting of chiral components with a low degree of asymmetry upon interaction with a chiral environment via a chirality transfer mechanism.

This phenomenon, termed supramolecular chirogenesis, is widely observed and plays a vital role in many natural systems such as the DNA double helix, the secondary α-helical structure of proteins, and heme proteins. Furthermore, this effect is extensively used in various artificial systems which are applied in the fields of asymmetric- and autocatalysis,[1] nonlinear optics,[2] polymer and material science,[3] molecular recognition and self-assembly,[4] and molecular device design.[5] In addition, the supramolecular chirogenesis has proved to be a useful tool in the determination of the absolute configuration of chiral compounds.[6]

Despite prominent current interest in this research area and a substantial increase in the number of publications on this subject, the detailed chirogenic mechanisms and influence of various factors controlling supramolecular chirality induction have not been well investigated and rationalized. Since noncovalent interactions are the basic key elements in this type of

(1) (a) Montanari, F.; Casella, L. *Metalloporphyrin Catalyzed Oxidations*; Kluwer: Dordrecht, 1994. (b) Seo, J. S.; Whang, D.; Lee, H.; Jun, S. I.; Oh, J.; Jeon, Y. J.; Kim, K. *Nature* **2000**, *404*, 982−986. (c) Nimri, S.; Keinan, E. *J. Am. Chem. Soc.* **1999**, *121*, 8978−8982. (d) Feringa, B. L.; van Delden, R. A. *Angew. Chem., Int. Ed.* **1999**, *38*, 3419−3438. (e) Lee, D. H.; Granja, J. R.; Martinez, J. A.; Severin, K.; Ghadiri, M. R. *Nature* **1996**, *382*, 525−528.

(2) (a) Verbiest, T.; Van Elshocht, S.; Kauranen, M.; Hellemans, L.; Snauwaert, J.; Nuckolls, C.; Katz, T. J.; Persoons, A. *Science* **1998**, *282*, 913−915. (b) Lin, W.; Wang, Z.; Ma, L. *J. Am. Chem. Soc.* **1999**, *121*, 11249−11250.

(3) (a) Jha, S. K.; Cheon, K.-S.; Green, M. M.; Selinger, J. V. *J. Am. Chem. Soc.* **1999**, *121*, 1665−1673. (b) Akagi, K.; Piao, G.; Kaneko, S.; Sakamaki, K.; Shirakawa, H.; Kyotani, M. *Science* **1998**, *282*, 1683−1686. (c) Yashima, E.; Maeda, K.; Okamoto, Y. *Nature* **1999**, *399*, 449−451. (d) Kepert, C. J.; Prior, T. J.; Rosseinsky, M. J. *J. Am. Chem. Soc.* **2000**, *122*, 5158−5168. (e) Jung, J. H.; Ono, Y.; Hanabusa, K.; Shinkai, S. *J. Am. Chem. Soc.* **2000**, *122*, 5008−5009. (f) Jung, J. H.; Ono, Y.; Shinkai, S. *Angew. Chem., Int. Ed.* **2000**, *39*, 1862−1865. (g) Lorenzo, M. O.; Baddeley, C. J.; Muryn, C.; Raval, R. *Nature* **2000**, *404*, 376−379. (h) Schaaff, T. G.; Whetten, R. L. *J. Phys. Chem. B* **2000**, *104*, 2630−2641. (i) Fuhrhop, J.-H.; Demoulin, C.; Boettcher, C.; Köning, J.; Siggel, U. *J. Am. Chem. Soc.* **1992**, *114*, 4159−4165.

(4) (a) Ogoshi, H.; Mizutani, T. *Acc. Chem. Res.* **1998**, *31*, 81−89. (b) James, T. D.; Sandanayake, K. R. A. S.; Shinkai, S. *Angew. Chem., Int. Ed.* **1996**, *35*, 1910−1922. (c) Prins, L. J.; Huskens, J.; de Jong, F.; Timmerman, P.; Reinhoudt, D. N. *Nature* **1999**, *398*, 498−502. (d) Nuckolls, C.; Hof, F.; Martin, T.; Rebek, J., Jr. *J. Am. Chem. Soc.* **1999**, *121*, 10281−10285. (e) Smith, J. O.; Olson, D. A.; Armitage, B. A. *J. Am. Chem. Soc.* **1999**, *121*, 2686−2695. (f) Ohkita, M.; Lehn, J.-M.; Baum, G.; Fenske, D. *Chem. Eur. J.* **1999**, *5*, 3471−3481. (g) Fan, J.; Whiteford, J. A.; Olenyuk, B.; Levin, M. D.; Stang, P. J.; Fleischer, E. B. *J. Am. Chem. Soc.* **1999**, *121*, 2741−2752. (h) Rivera, J. M.; Craig, S. L.; Martin, T.; Rebek, J., Jr. *Angew. Chem., Int. Ed.* **2000**, *39*, 2130−2132. (i) Mizuno, Y.; Aida, T.; Yamaguchi, K. *J. Am. Chem. Soc.* **2000**, *122*, 5278−5285. (j) Bellacchio, E.; Lauceri, R.; Gurrieri, S.; Scolaro, L. M.; Romeo, A.; Purrello, R. *J. Am. Chem. Soc.* **1998**, *120*, 12353−12354. (k) Takeuchi, M.; Imada, T.; Shinkai, S. *Angew. Chem., Int. Ed.* **(b) 1998**, *37*, 2096−2099. (l) Kikuchi, Y.; Tanaka, Y.; Sutarto, S.; Kobayashi, K.; Toi, H.; Aoyama, Y. *J. Am. Chem. Soc.* **1992**, *114*, 10302−10306.

(5) (a) Furusho, Y.; Kimura, T.; Mizuno, Y.; Aida, T. *J. Am. Chem. Soc.* **1997**, *119*, 5267−5268. (b) Feringa B. L.; van Delden, R. A.; Koumura, N.; Geertsema, E. M. *Chem. Rev.* **2000**, *100*, 1789−1816. (c) Zahn, S.; Canary, J. W. *Science* **2000**, *288*, 1404−1407.

10.1021/ja0032982 CCC: $20.00 © 2001 American Chemical Society
Published on Web 03/08/2001

chirality generation, there are several external (temperature, concentration, pH, polarity, viscosity, light) and internal (bonding strength, steric and electronic effects) factors which may affect these interactions and, in turn, the total chirality induction process. The first set of factors controlling the chiroptical properties in different supramolecular systems has recently been intensively studied. There are reports of solvent and temperature effects on helical oligomers,[7a−d] optically active liquid crystals,[7e] sexithiophenes[7f] and phthalocyanine[7g] aggregates, peptidic pseudorotaxanes,[7h] copper-containing polymers,[7i] and trimeric porphyrins.[7j] Other examples include ionic strength[8a] and pH[8b] dependencies of chiral porphyrin aggregates, host−guest stoichiometry dependence on the optical activity of a chiral tweezer,[9] stirring-induced chirality in porphyrin aggregates,[10] and light-controlled asymmetry in helical polymers,[11a] liquid crystals,[11b] and cobaloxime complex crystals.[11c] Recently, we have also discovered that temperature may serve as an effective tool to control supramolecular chirality induction in bis(zinc porphyrin) (**1**, see Figure 1) through the enhancement of ligand binding properties at low temperature.[6a]

In contrast to the external chirality-inducing factors which can affect various physicochemical properties of supramolecular systems concurrently, and thus produce an overall chiral state generated by multiple responses, the second set of the above-mentioned parameters, the internal chirality-inducing factors can be independently varied to study their effect on the chirogenetic processes. This is especially true for the systems where chromophores are spatially fixed, and hence their optical properties can be easily predicted. For example, in the case of covalently linked bis-chromophoric compounds, a clear dependence of the optical activity on their spatial arrangement was established theoretically and supported experimentally.[12] However, for noncovalently linked assemblies, this type of structure−activity relationship has not yet been well established, due to the difficulties in evaluation of spatial structures for most supramolecular systems. As for experimental studies, there are a number of reports on this subject, such as the interaction of different chiral guests with helical oligomers[13a] and bilindones,[13b,c] although a clear and unambiguous dependence between the guest structure and the efficiency of chirality induction in these systems has not been determined. Therefore, the study of this aspect is one of the "hottest" areas in current research.

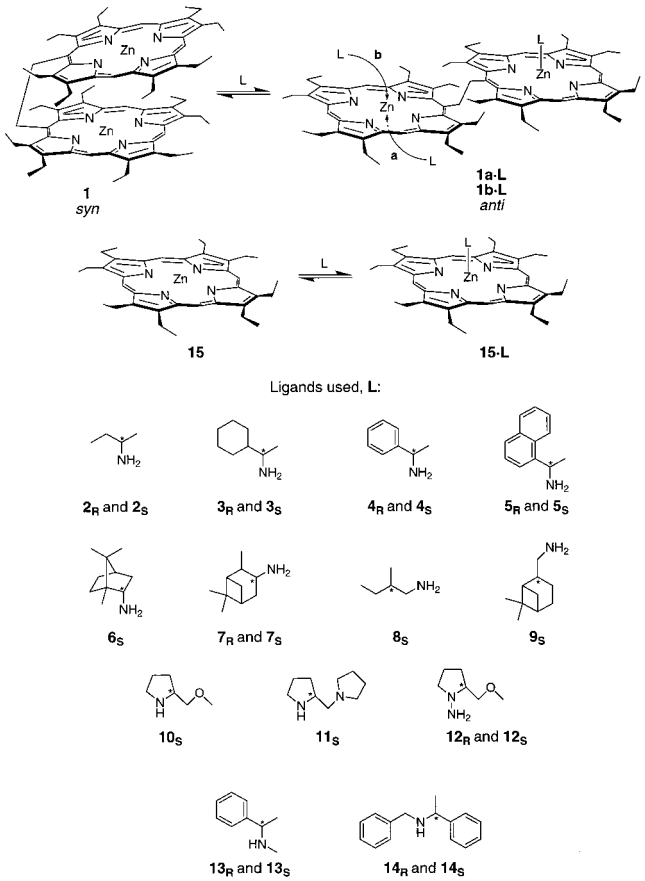

Figure 1. Structures and equilibria of achiral dimeric and monomeric hosts (**1** and **15**, respectively) in the presence of the enantiopure amine guests (**L**:**2**−**14**). For the second ligation step in the case of **1**, there are two possible approaches of **L**: **a**, symmetrical approach from the opposite face and **b**, asymmetrical approach from the same face. The subscript ($_R$ or $_S$) indicates the absolute configuration of the asymmetric carbon (marked by asterisk) which is the closest to the amine binding group.

We report here systematic studies of the roles of the chiral ligand structure (particularly, bulkiness at the chiral center and binding site, and relative position of the asymmetric carbon) and absolute configuration in the chirality-induction process in the porphyrin host **1** by CD, UV−vis, and ^{1}H NMR spectroscopies.[14]

Experimental Section

Materials. The *syn* conformer of host **1** in which the two porphyrin planes are fixed in a face-to-face orientation (see Figure 1) was synthesized according to previously reported methods.[15] Chiral amines

(6) (a) Borovkov, V. V.; Lintuluoto, J. M.; Fujiki, M.; Inoue, Y. *J. Am. Chem. Soc.* **2000**, *122*, 4403−4407. (b) Reuter, C.; Mohry, A.; Sobanski, A.; Vögtle, F. *Chem. Eur. J.* **2000**, *6*, 1674−1682. (c) Huang, X.; Borhan, B.; Rickman, B. H.; Nakanishi, K.; Berova, N. *Chem. Eur. J.* **2000**, *2*, 216−224. (d) Tsukube, H.; Shinoda, S. *Enantiomer* **2000**, *5*, 13−22. (e) Baum, G.; Constable, E. C.; Fenske, D.; Housecroft, C. E.; Kulke, T. *Chem. Eur. J.* **1999**, *5*, 1862−1873. (f) Huang, X.; Rickman, B. H.; Borhan, B.; Berova, N.; Nakanishi, K. *J. Am. Chem. Soc.* **1998**, *120*, 6185−6186. (g) Yashima, E.; Matsushima, T.; Okamoto, Y. *J. Am. Chem. Soc.* **1997**, *119*, 6345−6359. (h) Kikuchi, Y.; Kobayashi, K.; Aoyama, Y. *J. Am. Chem. Soc.* **1992**, *114*, 1351−1358.

(7) (a) Gin, M. S.; Moore, J. S. *Org. Lett.* **2000**, *2*, 135−138. (b) Prince, R. B.; Brunsveld, L.; Meijer, E. W.; Moore, J. S. *Angew. Chem., Int. Ed.* **2000**, *39*, 228−230. (c) Cheon, K. S.; Selinger, J. V.; Green, M. M. *Angew. Chem., Int. Ed.* **2000**, *39*, 1482−1485. (d) Fujiki, M. *J. Am. Chem. Soc.* **2000**, *122*, 3336−3343. (e) Serrano, J. L.; Sierrs, T. *Chem. Eur. J.* **2000**, *6*, 759−766. (f) Kilbinger, A. F. M.; Schenning, A. P. H. J.; Goldoni, F.; Feast, W. J.; Meijer, E. W. *J. Am. Chem. Soc.* **2000**, *122*, 1820−1821. (g) Fox, J. M.; Katz, T. J.; Elshocht, S. V.; Verbiest, T.; Kauranen, M.; Persoons, A.; Thongpanchang, T.; Krauss, T.; Brus, L. *J. Am. Chem. Soc.* **1999**, *121*, 3453−3459. (h) Meillon, J.-C.; Voyer, N.; Biron, E.; Sanschagrin, F.; Stoddart, J. F. *Angew. Chem., Int. Ed.* **2000**, *39*, 143−145. (i) Ranford, J. D.; Vittal, J. J.; Wu, D.; Yang, X. *Angew. Chem., Int. Ed.* **1999**, *38*, 3498−3501. (j) Arai, T.; Takei, K.; Nishino, N.; Fujimoto, T. *Chem. Commun.* **1996**, 2133-2134.

(8) (a) Fukushima, Y. *Bull. Chem. Soc. Jpn.* **1996**, *69*, 1719−1726. (b) Purrello, R.; Bellacchio, E.; Gurrieri, S.; Lauceri, R.; Raudino, A.; Scolaro, L. M.; Santoro, A. M. *J. Phys. Chem. B* **1998**, *102*, 8852−8857.

(9) Matsui, H.; Kushi, S.; Matsumoto, S.; Akazome, M.; Ogura, K. *Bull. Chem. Soc. Jpn.* **2000**, *73*, 991−997.

(10) Rubires, R.; Crusats, J.; El-Hachemi, Z.; Jaramillo, T.; López, M.; Valls, E.; Farrera, J.-A.; Ribó, J. *New. J. Chem.* **1999**, 189−198.

(11) (a) Li, J.; Schuster, G. B.; Cheon, K.-S.; Green, M. M.; Selinger, J. V. *J. Am. Chem. Soc.* **2000**, *122*, 2603−2612. (b) Burnham, K. S.; Schuster, G. B. *J. Am. Chem. Soc.* **1999**, *121*, 10245−10246. (c) Nemoto, T.; Ohashi, Y. *Bull. Chem. Soc. Jpn.* **1999**, *72*, 1971−1983.

(12) Harada, N.; Nakanishi, K. *Circular Dichroic Spectroscopy. Exciton Coupling in Organic Stereochemistry*; University Science Books: Mill Valley, CA, 1983.

(13) (a) Prince, R. B.; Barnes, S. A.; Moore, J. S. *J. Am. Chem. Soc.* **2000**, *122*, 2758−2762. (b) Mizutani, T.; Yagi, S.; Honmaru, A.; Murakami, S.; Furusyo, M.; Takagishi, T.; Ogoshi, H. *J. Org. Chem.* **1998**, *63*, 8769−8784. (c) Mizutani, T.; Yagi, S.; Honmaru, A.; Ogoshi, H. *J. Am. Chem. Soc.* **1996**, *118*, 5318−5319.

(14) For preliminary account of the part of this work related to the bulkiness effect at the chiral center see: Borovkov, V. V.; Lintuluoto, J. M.; Inoue, Y. *Org. Lett.* **2000**, *2*, 1565−1568.

2−**14** and (octaethylporphyrinato)zinc (**15**) shown in Figure 1, anhydrous CH_2Cl_2 for UV−vis and CD measurements, and $CDCl_3$ for ^1H NMR studies were purchased from Fluka Chemica AG and Aldrich Chemical Co. and used as received.

Spectroscopic Measurements. UV−vis and CD spectra were measured at room temperature on a Shimadzu UV-3101PC spectrometer and JASCO J-720 spectropolarimeter, respectively. CD scanning conditions were as follows: scanning rate = 50 nm per min, bandwidth = 1 nm, response time = 0.5 s, accumulations = 1 time. The saturated amine concentrations used for the UV−vis and CD measurements were the concentrations where the spectral changes associated with the porphyrin chromophores were at their maximum, and further increase of the amine concentration had no effect on the signal intensities (for the amine and porphyrin concentration ranges, see footnote a in Tables 1 and 2).

^1H NMR spectra were recorded at 400 MHz on a JEOL JNM-EX 400 spectrometer at 243 K (for the amine and porphyrin concentration ranges, see footnote a in Table 3). Chemical shifts were referenced to the residual proton resonance in $CDCl_3$ (δ 7.25 ppm).

Results and Discussion

1. Supramolecular Systems. Bis-porphyrin **1**[15] which is connected by a short covalent bridge (Figure 1) has been chosen as an achiral host molecule. This compound is well-suited for the study of supramolecular chirality induction processes because of the clear and easily observable spectral differences between the initial noninteracting form (*syn* **1**) and the final ligand-bonded form (*anti* **1**).[16] That is, in turn, a result of the unique properties of **1** to exist in a folded *syn* (face-to-face) conformation in nonpolar solvents due to strong intramolecular $\pi-\pi$ interactions between the two zinc porphyrin macrocycles, and then to switch to an extended *anti* form upon complexation with the external ligands.

Amines have been chosen as chiral guests because of their well-known ability to coordinate to zinc porphyrins and to form stable coordinated adducts at room temperature.[17] To investigate the influence of different structural factors on supramolecular chirogenesis in **1**, various commercially available amines **2**−**14**, shown in Figure 1, have been used as external ligands in this study. These guests can be classified into several structurally homologous categories: type A is the α-substituted ethylamines (**2**−**5**) distinguished by the size of the substituent (X) at the asymmetric carbon (C*) with the general chemical formula XC*H(Me)NH_2, type B is the cyclic amines (**6**, **7**), type C is the cyclic secondary amines (pyrrolidine derivatives **10**, **11**), type D is the compounds (**8**, **9**, **12**), where an asymmetric carbon is at the β-position to the amine binding group separated by a methylene (in the case of **8** and **9**) or tertiary amine (in the case of **12**) group, and type E is the ligands (**4**, **13**, **14**) distinguished by the size of the N-substituent (R) with the general chemical formula PhC*H(Me)NHR (R = H, Me, and Bzl for **4**, **13**, and **14**, respectively). These homologous categories cover the most important structural modification of the guest molecules.[18]

However, since the achiral host **1** consists of two porphyrin macrocycles, the direct interactions between each porphyrin and the enantiopure ligands can lead to chirality induction at the unimolecular level (point chirality effect) as well, due to chiral deformations within a single porphyrin moiety rather than within the whole supramolecular system. To elucidate the point chirality contribution to the total chirality induction and to separate it from the supramolecular chirogenesis phenomenon, interactions of the monomeric host **15** with several chiral amines have been investigated first.

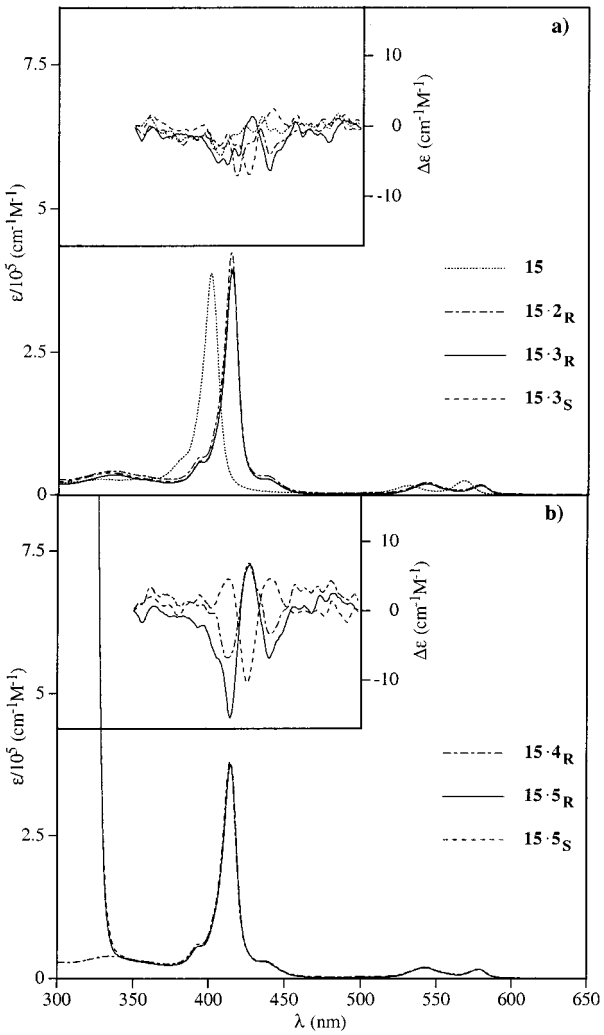

Figure 2. UV−vis and CD (inset) spectra of **15** in CH_2Cl_2 at 292 K without ligands and in the presence of different chiral amines.

2. Point Chirality Induction in The Monomeric Host 15. Interactions between the monomeric host **15** and various chiral amines **2**−**5** were examined by UV−vis and CD spectroscopy.

2.1. UV−Vis Spectral Changes. All of the UV−vis spectra of the complexes of **15** with **2**−**5** show almost the same spectral pattern, which is different from that of the spectrum of uncomplexed **15** (Figure 2, Table 1). These spectral changes are associated with the ligation process. Thus, at the amine-saturated concentration, where the 1:1 host−guest complex is formed due to the pentacoordinate properties of zinc porphyrins,[17,19] the position of the Soret band (corresponding to the porphyrin B transition) and visible bands (corresponding to the porphyrin Q transitions) are bathochromically shifted by 11−14 nm. This low-energy shift is a result of amine coordination on the zinc porphyrin and consequent p_z-a_{2u} ligand−porphyrin

(15) (a) Borovkov, V. V.; Lintuluoto, J. M.; Inoue, Y. *Synlett* **1998**, 768−770. (b) Borovkov, V. V.; Lintuluoto, J. M.; Inoue, Y. *Helv. Chim. Acta* **1999**, *82*, 919−934.

(16) (a) Borovkov, V. V.; Lintuluoto, J. M.; Inoue, Y. *Tetrahedron Lett.* **1999**, *40*, 5051−5054. (b) Borovkov, V. V.; Lintuluoto, J. M.; Inoue, Y. *J. Phys. Chem. B* **1999**, *103*, 5151−5156.

(17) Smith, K. M. *Porphyrins and Metalloporphyrins*; Elsevier: Amsterdam, 1975.

(18) Investigation of supramolecular chirality induction using an essentially different type of structural modification by changing the binding functional group of the chiral guests is currently in progress and will be reported elsewhere.

(19) Detailed equilibria, binding parameters, and thermodynamics of the complexation and chirality induction processes in dimeric and monomeric hosts (**1** and **15**, respectively) upon interaction with chiral amines will be reported elsewhere: Borovkov, V. V.; Lintuluoto, J. M.; Sugeta, H.; Fujiki, M.; Inoue, Y. Manuscript in preparation.

Table 1. UV−Vis and CD Spectral Data of **15** and the Resulting System **15·L** with Different Chiral Amines[a]

	UV−vis data λ_{max} (nm) [$\epsilon/10^5$ (M^{-1} cm^{-1})]	CD data λ_{max} (nm) [$\Delta\epsilon_n$ (M^{-1} cm^{-1})]			
system	B transition	first Cotton ($n = 1$)	second Cotton ($n = 2$)	third Cotton ($n = 3$)	$\lvert A\rvert$[b]
15	401 [3.86]	–	–	–	–
15·2$_R$	414 [4.24]	–	–	–	–
15·2$_S$	414 [3.88]	–	–	–	–
15·3$_R$	415 [3.93]	439 [−6.32]	427 [+1.43]	–	−7.75
15·3$_S$	415 [4.01]	441 [+2.50]	425 [−6.83]	–	+9.33
15·4$_R$	414 [3.80]	440 [−3.31]	426 [+7.00]	412 [−6.75]	−10.31
15·4$_S$	414 [3.77]	441 [+6.71]	425 [−6.28]	414 [+6.75]	+12.99
15·5$_R$	414 [3.75]	440 [−6.84]	427 [+6.73]	414 [−15.45]	−13.57
15·5$_S$	414 [3.79]	441 [+4.74]	425 [−10.34]	412 [+4.70]	+15.08

[a] $C_{15} = 2.6-2.7\cdot10^{-6}$ M, $C_L = 2.5-4.0\cdot10^{-1}$ M in CH_2Cl_2. [b] $|A| = \Delta\epsilon_1 - \Delta\epsilon_2$. This value represents the total amplitude of the CD couplets.

orbital mixing. This effect is well-known and reported for various monomeric zinc porphyrins.[17,20]

2.2. CD Spectral Changes. In contrast to similar absorption properties, the optical activities of these complexes are rather different. Particularly, while the free **15** and both complexes **15·2$_R$** and **15·2$_S$** are CD silent (or at least in the latter case the CD signal cannot be detected against the background of measurements), the CD signals of small intensities but clearly visible in the spectral region associated with the porphyrin B transition are observed for the other complexes **15·3**−**15·5** (Figure 2, Table 1). The aliphatic amine-containing systems **15·3** exhibit two small Cotton effects (the total CD amplitude $|A| < 10$ M^{-1} cm^{-1}) which are red-shifted in comparison to the B transition defined in the UV−vis spectra. In the case of the aromatic complexes **15·4** and **15·5**, besides the same two Cotton effects with slightly larger intensities ($|A| = 10-15$ M^{-1} cm^{-1}), there is the third Cotton effect with comparable intensity and extremum matched to the absorption Soret band. The induced chirality in the monomeric **15** arises obviously from coordination of the chiral amines to the central zinc ion of the porphyrin core.[21] The induced optical activity caused by asymmetry transfer from the enantiopure ligand to inherently symmetrical porphyrin may be observed as a result of the direct excitonic coupling between porphyrin and ligand electronic transitions (for aromatic amines **4** and **5**) and conformational distortion of the porphyrin plane due to the ligation process (for all amines), resulting in symmetry breaking. Indeed, although the CD signals of these systems are rather small, it can be seen that the Cotton effects of the aromatic-containing **15·4** and **15·5** give relatively more intense signals, indicating that the former factor can play a greater role for these complexes. Furthermore, additional $\pi-\pi$ interactions between the ligand aromatic substituents and porphyrin ring may restrict the free rotation about the coordination Zn−N (N of the ligand) bond, reducing the number of possible conformations. This must be an important factor controlling the chirality induction process, since conformers with the spatially opposite orientation of the interacting transition dipoles apparently have inverted signs of the induced Cotton effects,[12] which in turn results in decrease or even disappearance (as probably in the case of **15·2**) of the overall CD signal intensity of the averaged system.

One of the first observations of chirality induction in optically inactive monomeric metalloporphyrins upon coordination of the amino acids was done by Choon and Rodley[22] in 1983. It was shown that the induced Cotton effects are dependent upon ligand−metalloporphyrin interactions; however, the mechanism of asymmetry transfer was not presented. The most thorough and complete up-to-date investigation of chirality induction in monomeric metalloporphyrins was carried out by Mizutani and Ogoshi.[4,23] The possible mechanisms of the induced circular dichroism were suggested and analyzed in detail. These included both the coupling between the electronic transitions of the aromatic groups and porphyrin ring, and puckering of the porphyrin plane caused by complexation with chiral ligands. Other studies related to the chirality induction in monomeric porphyrins were done by Hsu and Woody,[24a] and Benson et al.[24b] who demonstrated the importance of the amino acid aromatic substituents for the induced CD signals observed in hemoproteins, as well as by Aida et al.[5] who reported distinct CD signals with the split Cotton effects of individual nonplanar porphyrin conformers discriminated upon hydrogen bonding with optically active carboxylic acids.

Our results on chirality induction in the monomeric **15** by the chiral amines **2**−**5** are in good agreement with the reported literature data and show clearly that the point chirality effect as shown below can have a small contribution to optical activity of the whole supramolecular system.

3. Supramolecular Chirality Induction in Bis-porphyrin Host 1. Taking into account the point chirality effect due to direct interactions between monomeric metalloporphyrin and chiral ligands, the supramolecular chirality induction phenomenon in the bis-porphyrin host **1** was studied in the presence of enantiopure guests by means of UV−vis, CD, and ^{1}H NMR spectroscopy. These methods revealed dramatic transformations from the initial spectral pattern of the *syn* form **1** upon interaction with chiral amines **2**−**14**.

3.1. UV−Vis Spectral Changes. In the UV−vis spectra of all the systems **1·2**−**1·14** studied there are common special features which are attributable to the *anti* conformation of the bis-porphyrin host **1** that differ drastically from the spectral pattern of the initial *syn* **1**. These include an intense, bathochromically shifted, well-resolved, and split Soret band in the region of 425−438 nm which is associated with the two $B_\perp$ and $B_{||}$ transitions (which are correspondingly in perpendicular and parallel orientations to the axis connecting two intramolecular porphyrin rings[16]); low-intensity Q_{X00} and Q_{X01} bands

(20) (a) Kirksey, C. H.; Hambright, P.; Storm, C. B. *Inorg. Chem.* **1969**, *8*, 2141−2144. (b) Miller, J. R.; Dorough, G. D. *J. Am. Chem. Soc.* **1952**, *74*, 3977−3976.

(21) Since the approach of the chiral amines **2**−**5** to monomeric **15**, and rotation about the Zn−N coordination bond apparently are not sterically hindered, the induced chirality in the complexes **15·3**−**15·5** is a sum of the CD spectra of the differently orientated rotamers.

(22) (a) Choon, O. C.; Rodley, G. A. *Inorg. Chim. Acta* **1983**, *80*, 177−182. (b) Choon, O. C.; Rodley, G. A. *Origins Life* **1984**, 427−431.

(23) (a) Mizutani, T.; Ema, T.; Yoshida, T.; Kuroda, Y.; Ogoshi, H. *Inorg. Chem.* **1993**, *32*, 2072−2077. (b) Mizutani, T.; Ema, T.; Yoshida, T.; Renné, T.; Ogoshi, H. *Inorg. Chem.* **1994**, *33*, 3558−3566. (c) Mizutani, T.; Murakami, S.; Kurahashi T.; Ogoshi, H. *J. Org. Chem.* **1996**, *61*, 539−548.

(24) (a) Hsu, M.-C.; Woody, R. W. *J. Am. Chem. Soc.* **1971**, *93*, 3515−3525. (b) Liu, D.; Williamson, D. A.; Kennedy, M. L.; Williams, T. D.; Morton, M. M.; Benson, D. R. *J. Am. Chem. Soc.* **1999**, *121*, 11798−11812.

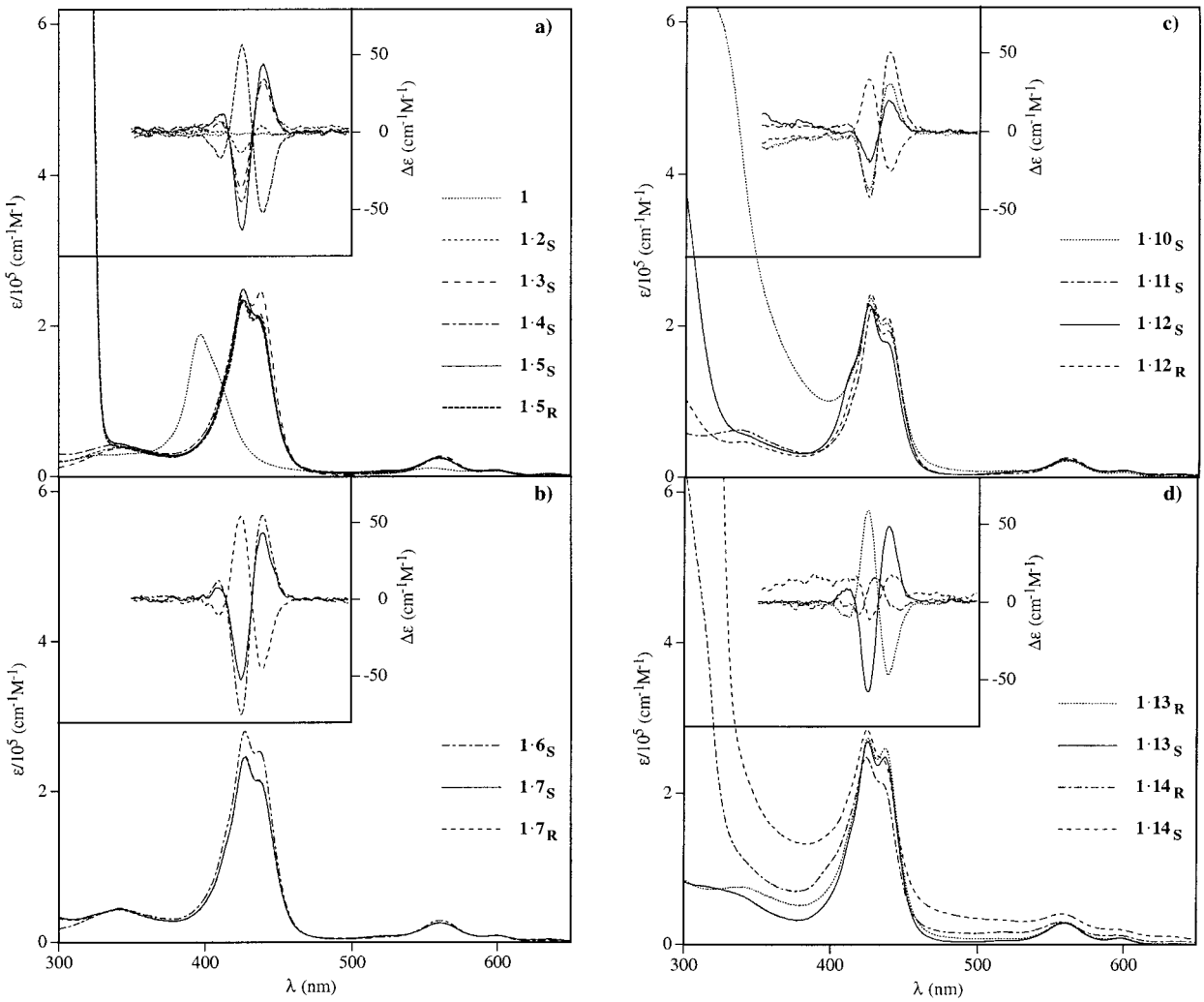

Figure 3. UV−vis and CD (inset) spectra of **1** in CH_2Cl_2 at 292 K without ligands and in the presence of different chiral amines.

in the region of 560−600 nm with substantial enhancement of the Q_{X01} transition intensity in comparison to the Q_{X00} transition (while for *syn* **1** the intensities of Q_{X00} and Q_{X01} bands are almost the same); and a high-energy transition associated with the ligand coordination on metalloporphyrins (Figure 3, Table 2).[25] These UV−vis spectral changes are a result of the same *syn*−*anti* conformational switching induced by external ligation as described for achiral[16] and chiral[6a] guests at low temperature. It is noteworthy that the shape, positions, and intensities of the UV−vis bands of *anti* **1·L** (**L = 2−14**) are almost the same regardless of the structure of the amine used.

The remarkable Soret band splitting ($\Delta\lambda = 10-12$ nm), which is caused by nonequivalent coupling of the two degenerate B transitions (Davydov splitting), is in good agreement with exciton coupling theory[26] and previously reported data for different bis- and multi-porphyrins with extended edge-to-edge spatial orientation.[27] This effect and its application to the systems *anti* **1·L** have been previously described in detail.[16]

3.2. CD Spectral Changes. While the parent *syn* **1** is intrinsically achiral and hence CD silent, all of the supramolecular systems *anti* **1·L** show remarkable optical activity in the region of the porphyrin Soret band, giving the two major bisignate Cotton effects (Figure 3, insets). The positions of the first and second Cotton effects coincide very closely with the maxima of the split Soret band which are well-resolved in the

(25) Besides the listed UV−vis spectral features, there is another intensive absorption at the high energy region of the spectra of **1·5**, **1·10**, **1·12**, **1·14** apparently associated with the absorption of either the amine itself or impurities contained in the commercial samples.

(26) Kasha, M.; Rawls, H. R.; El-Bayoumi, M. A. *Pure Appl. Chem.* **1965**, *11*, 371−392.

(27) (a) Arnold, D. P. *Synlett* **1999**, 296−305. (b) Anderson, H. L. *Chem. Commun.* **1999**, 2323−2330. (c) Kuciauskas, D.; Liddell, P. A.; Lin, S.; Johnson, T. E.; Weghorn, S. J.; Lindsey, J. S.; Moore, A. L.; Moore, T. A.; Gust, D. *J. Am. Chem. Soc.* **1999**, *121*, 8604−8614. (d) Ruhlmann, L.; Lobstein, S.; Gross, M.; Giraudeau, A. *J. Org. Chem.* **1999**, *64*, 1352−1355. (e) Ogawa, T.; Nishimoto, Y.; Yoshida, N.; Ono, N.; Osuka, A. *Angew. Chem., Int. Ed.* **1999**, *38*, 176−179. (f) Ponomarev, G. V.; Yashunsky, D. V.; Borovkov, V. V.; Sakata, Y.; Arnold, D. *Russ. Chem. Heterocycl. Cmpd.* **1997**, 1627. (g) Chernook, A. V.; Shulga, A. M.; Zenkevich, E. I.; Rempel, U.; von Borczyckowski, C. *J. Phys. Chem.* **1996**, *100*, 1918. (h) Zhou, X.; Chan, K. S. *J. Org. Chem.* **1998**, *63*, 99. (i) Zhou, X.; Chan, K. S. *J. Chem. Soc., Chem. Commun.* **1994**, 2493. (j) Sessler, J. L.; Capuano, V. L. *Tetrahedron Lett.* **1993**, *34*, 2387. (k) Osuka, A.; Tanabe, N.; Zhang, R.-P.; Maruyama, K. *Chem. Lett.* **1993**, 1505. (l) Shultz, D. A.; Gwaltney, K. P.; Lee, H. *J. Org. Chem.* **1998**, *63*, 4034. (m) Arnold, D. P.; Heath, G. A.; James, D. A. *New J. Chem.* **1998**, 1377. (n) Arnold, D. P.; James, D. A. *J. Org. Chem.* **1997**, *62*, 3460. (o) Arnold, D. P.; James, D. A.; Kennard, C. H. L.; Smith, G. *J. Chem. Soc., Chem. Commun.* **1994**, 2131. (p) Arnold, D. P.; Heath, G. A. *J. Am. Chem. Soc.* **1993**, *115*, 12197. (q) Lin, V. S.-Y.; DiMagno, S. G.; Therien, M. J. *Science* **1994**, *264*, 1105. (r) Anderson, H. L. *Inorg. Chem.* **1994**, *33*, 972. (s) Higuchi, H.; Shimizu, K.; Takeuchi, M.; Ojima, J.; Sugiura, K.-i.; Sakata, Y. *Bull. Chem. Soc. Jpn.* **1997**, *70*, 1923. (t) Higuchi, H.; Takeuchi, M.; Ojima, J. *Chem. Lett.* **1996**, 593. (u) Kitagawa, R.; Kai, Y.; Ponomarev, G. V.; Sugiura, K.-i.; Borovkov, V. V.; Kaneda, T.; Sakata, Y. *Chem. Lett.* **1993**, 1071. (v) Yoshida, N.; Shimidzu, H.; Osuka, A. *Chem. Lett.* **1998**, 55. (w) Kuroda, Y.; Shiraishi, N.; Sugou, K.; Sasaki, K.; Ogoshi, H. *Tetrahedron Lett.* **1998**, *39*, 2993. (x) Sessler, J. L.; Johnson, M. R.; Lin, T.-Y.; Creager, S. E. *J. Am. Chem. Soc.* **1988**, *110*, 3659. (y) Tabushi, I.; Kugimiya, S.-i.; Kinnaird, M. G.; Sasaki, T. *J. Am. Chem. Soc.* **1985**, *107*, 4192.

Table 2. UV−Vis and CD Spectral Data of **1** and the Resulting Supramolecular System **1·L** with Different Chiral Amines[a]

	UV−vis data λ_{max} (nm) [$\epsilon/10^5$ (M^{-1} cm^{-1})]		CD data λ_{max} (nm) [$\Delta\epsilon_n$ (M^{-1} cm^{-1})]			
system	$B_{\|\|}$ transition	$B_{\perp}$ transition	first Cotton ($n = 1$)	second Cotton ($n = 2$)	third Cotton ($n = 3$)[b]	$\|A\|$[c]
1	397[1.89][d]		–	–	–	–
1·2$_R$	437 [2.18]	426 [2.26]	440 [−12.9]	426 [+7.6]	–	−20.5
1·2$_S$	437 [2.17]	426 [2.32]	438 [+4.5]	425 [−13.5]	–	+18.0
1·3$_R$	438 [2.53]	427 [2.52]	439 [−33.1]	425 [+39.6]	411 [−5.6]	−72.7
1·3$_S$	438 [2.46]	427 [2.46]	439 [+31.7]	425 [−36.1]	411 [+6.7]	+67.8
1·4$_R$	436 [2.11]	426 [2.26]	439 [−42.0]	425 [+42.1]	410 [−11.2]	−84.1
1·4$_S$	436 [2.12]	426 [2.35]	439 [+33.7]	425 [−44.7]	410 [+8.2]	+78.4
1·5$_R$	436 [2.12]	426 [2.35]	439 [−51.2]	426 [+56.7]	411 [−16.3]	−107.9
1·5$_S$	436 [2.14]	426 [2.50]	439 [+44.5]	426 [−63.2]	412 [+12.2]	+107.7
1·6$_S$	437 [2.54]	427 [2.81]	439 [+54.8]	425 [−74.9]	410 [+12.6]	+129.7
1·7$_R$	436 [2.16]	426 [2.47]	439 [−44.7]	426 [+54.2]	410 [−10.3]	−98.9
1·7$_S$	436 [2.14]	426 [2.46]	439 [+43.5]	425 [−52.3]	410 [+7.8]	+95.8
1·8$_S$	437 [2.41]	426 [2.63]	438 [+4.0]	426 [−7.9]	–	+11.9
1·9$_S$	437 [1.93]	427 [2.25]	437 [+4.5]	424 [−2.7]	–	+7.2
1·10$_S$	437 [2.04]	426 [2.36]	439 [+30.8]	425 [−37.0]	–	+67.8
1·11$_S$	438 [1.94]	427 [2.24]	439 [+50.6]	425 [−42.1]	–	+92.7
1·12$_R$	437 [2.12]	426 [2.43]	439 [−25.6]	424 [+33.5]	–	−59.1[e]
1·12$_S$	436 [1.80]	425 [2.28]	438 [+20.3]	425 [−19.5]	–	+39.8[e]
1·13$_R$	437 [2.61]	426 [2.74]	438 [−46.8]	425 [+59.4]	411 [−9.7]	−106.2
1·13$_S$	437 [2.49]	426 [2.69]	438 [+50.0]	425 [−57.7]	410 [+9.0]	+107.7
1·14$_R$[f]	435 [2.14]	425 [2.48]	446 [−5.0]	429 [+16.4]	418 [−8.0]	−21.4[e]
1·14$_S$[f]	435 [2.47]	425 [2.85]	440 [+17.9]	426 [−11.4]	417 [+17.1]	+29.3[e]

[a] $C_1 = 2.9-3.8\cdot10^{-6}$ M, $C_L = 3.5\cdot10^{-2} - 4.7\cdot10^{-1}$ M in CH_2Cl_2. [b] The third relatively small Cotton effect is likely to result from a point chirality phenomenon that may include a conformational distortion of the porphyrin plane due to ligation process and excitonic coupling between porphyrin B and the ligand's aromatic dipoles (in the case of aromatic amines). [c] $|A| = \Delta\epsilon_1 - \Delta\epsilon_2$. This value represents the total amplitude of the CD couplets. The CD recording accuracy based on the baseline evaluation is ±3 M^{-1} cm^{-1}. [d] There is no split of B band. [e] The considerable deviations of the *A* value for corresponding enantiomers are due to purity difference between the purchased *R* and *S* amine. [f] $C_L = 1.0$ M in CH_2Cl_2.

UV−vis spectra and associated with the allowed $B_{||}$ and $B_{\perp}$ electronic transitions, respectively (Table 2). Therefore, it is assumed that these transitions are the major contributors to the observed CD couplets. Interestingly, there is the same good match between the observed CD splitting and sharply defined Davydov splitting of the Soret band for different *anti* **1·L** at low temperature that was reported previously.[6a] Although coupled chromophores which are arranged in a chiral spatial orientation are normally expected to exhibit bisignate CD couplets due to excitonic coupling between their electronic transitions,[12] there are only a few examples[28] of such a good match between the CD split and the Davydov split observed in the UV−vis spectra.

In contrast to the UV−vis spectra, the intensity and signs of the induced CD signals of *anti* **1·L** are strongly dependent on the ligand structure (Figure 3, insets; Table 2). The general tendencies are as follows. Amines with aromatic or cyclic aliphatic substituents at the asymmetric carbon produce 4−7 times more intensive Cotton effects than the ligands with acyclic aliphatic substituents. Amines with the chiral center at the β-position with respect to the amino group show a considerable decrease in the CD signal. Substitution at the amino group exhibits a dual effect. Methyl substitution (in the case of **13**) results in moderate enhancement of the CD amplitude (1.3−1.4 times), while insertion of the benzyl group (in the case of **14**) reduces the $|A|$ value greatly (2.7−3.9 times). The sign of the CD couplet is directly dependent on the guest absolute configuration. Thus, all of the (*R*)-enantiomers give a negative first Cotton effect and positive second Cotton effect, while the guests with the *(S)* absolute configuration produce CD signals with opposite signs, yielding the corresponding mirror images.[29]

3.3. ^{1}H NMR Spectral Changes. The ^{1}H NMR spectra were recorded at 243 K and at the **1** to **L** molar ratio of 1:5 to ensure the optimal measuring conditions and shift of the *syn* to *anti* equilibrium to give over 95% of the corresponding *anti* form. The spectral profiles of the complexes **1·2$_R$**, **1·4$_{R,S}$**, and **1·5$_R$** differ significantly from the initial spectrum of **1** (Figure 4, Table 3). For all of these supramolecular systems the chemical shifts of the 10,20-*meso* protons ($H_{a,b}$ protons, see Figure 5) are shifted downfield considerably ($\Delta\delta = 1.78-1.9$ ppm), while the position of the 15-*meso* protons (H_c protons, see Figure 5) does not show any significant change upon interaction with the external ligands. Remarkably, in contrast to the systems containing achiral ligands[16] or chiral alkylamine **1·2$_R$**, the systems containing chiral aromatic amines **1·4$_{R,S}$** and **1·5$_R$** exhibit a split of the signal of the 10,20-*meso* protons into two singlets of equal intensities. Similar behavior is observed for the $-CH_2CH_2-$ bridge protons. Thus, their resonance is presented either as a moderately broad singlet which is shifted upfield ($\Delta\delta = 0.1$ ppm) in the case of **1·2$_R$** or as two multiplets, one of which is also shifted upfield ($\Delta\delta = 0.11-0.19$ ppm), while another is shifted downfield slightly ($\Delta\delta = -0.01$ to -0.19 ppm) in the cases of **1·4$_{R,S}$**, and **1·5$_R$**. The eight well-resolved signals of the $-C\underline{H}_2CH_3$ protons ($\delta = 4.30-2.38$ ppm) transform into several broad multiplets located at a more narrow

(28) Examples of systems with a good match between CD and Davydov splits: (a) Bari, L. D.; Pescitelli, G.; Salvadori, P. *J. Am. Chem. Soc.* **1999**, *121*, 7998−8004. (b) Gargiulo, D.; Ikemoto, N.; Odingo, J.; Bozhkova, N.; Berova, N.; Nakanishi, K. *J. Am. Chem. Soc.* **1994**, *116*, 3760−3767. (c) Gargiulo, D.; Cai, G.; Ikemoto, N.; Bozhkova, N.; Odingo, J.; Berova, N.; Nakanishi, K. *Angew. Chem., Int. Ed. Engl.* **1993**, *32*, 888−891. (d) Berova, N.; Gargiulo, D.; Derguini, F.; Nakanishi, K.; Harada, N. *J. Am. Chem. Soc.* **1993**, *115*, 4769−4775.

(29) Some deviations from the mirror image CD spectra for enantiomeric pairs of **1·2**−**1·5**, **1·7**, **1·13** (Table 2) are due to experimental errors in the CD scanning conditions (see, Experimental Section). More precise measurements (accumulations = 4 times and use of the same cell used for both enantiomers) give good mirror image CD spectra for the corresponding enantiomeric pairs with essentially unchanged $|A|$ values. For example, the first Cotton effect/second Cotton effect ratios are −7.9/+10.2 for **1·2$_R$** and +5.9/−12.3 for **1·2$_S$**, −37.3/+44.8 for **1·4$_R$** and +38.6/−45.0 for **1·4$_S$**, and −50.8/+64.1 for **1·5$_R$** and +51.0/−61.7 for **1·5$_S$**.

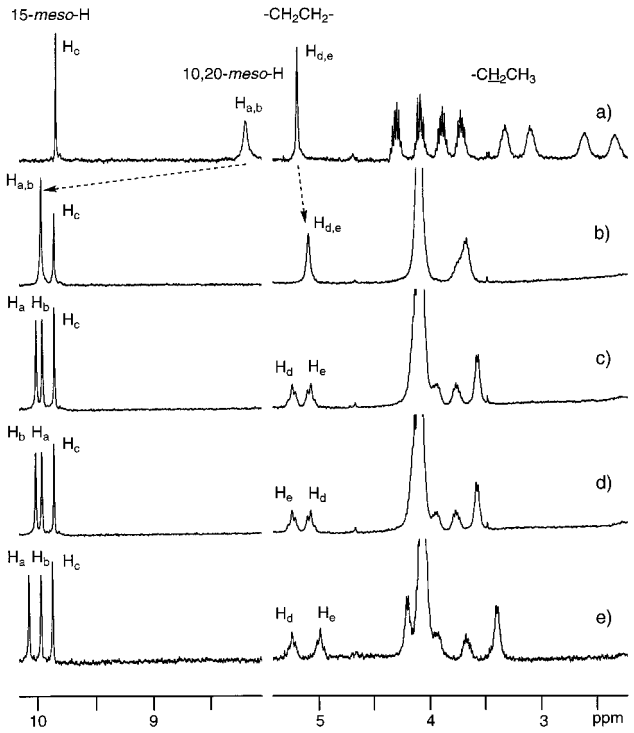

Figure 4. Selected areas of ^{1}H NMR spectra of **1** in $CDCl_3$ without ligands (a) at 293 K and in the presence of different chiral amines: **1·2$_R$** (b), **1·4$_R$** (c), **1·4$_S$** (d), **1·5$_R$** (c) at 243 K.

Table 3. ^{1}H NMR Spectral Data of **1** at 293 K and the Resulting Supramolecular Systems **1·L** at 243 K[a]

	chemical shift δ (ppm) (number of protons, multiplicity)		
system	10,20-*meso*-$H_{a,b}$	15-*meso*-H_c	$-CH_2CH_2-$bridge$-H_{d,e}$
1	8.18 (2H, br. s)	9.84 (2H, s)	5.17 (4H, s)
1·2$_R$	9.97 (4H, s)	9.85 (2H, s)	5.07 (4H, s)
1·4$_R$	10.01 (2H, s), 9.96 (2H, s)	9.85 (2H, s)	5.22 (2H, m), 5.06 (2H, m)
1·4$_S$	10.01 (2H, s), 9.96 (2H, s)	9.85 (2H, s)	5.22 (2H, m), 5.06 (2H, m)
1·5$_R$	10.08 (2H, s), 9.98 (2H, s)	9.88 (2H, s)	5.23 (2H, m), 4.98 (2H, m)

[a] $C_1 = 1.57-1.62\cdot10^{-3}$ M, $C_L = 7.85-8.10\cdot10^{-3}$ M in $CDCl_3$.

region ($\delta = 4.24-3.33$ ppm) with the center of these signals shifted downfield. These changes arise from the *syn*−*anti* conformational switching, which has been recently studied by VT ^{1}H NMR experiments with achiral alcohols[16] and chiral amines.[6a]

4. Mechanism of Supramolecular Chirality Induction in Bis-porphyrin 1. The observed spectral changes are in good agreement with the chirality induction mechanism in **1** in the presence of chiral ligands studied at low temperature and reported recently.[6a] This mechanism includes a stepwise ligation process leading to the *syn*−*anti* conformational switching. It was shown that the guest's interactions with the *syn* conformation of **1** result in the formation of the *anti* species after the first ligation.[16] Additionally, it was shown also by VT ^{1}H NMR experiments that **1·5$_R$** at the **1**-to-**L** molar ratio of 1:1 is in the *anti* conformation at 233 K in $CDCl_3$. Since there are two porphyrin rings in **1**, the presence of a large excess of the amine (see footnote a of Table 2) results in obvious second ligation step,[19] which was also proved by an excellent theoretical fit of the experimental data obtained previously for **1·L**, where **L** were achiral alcohols.[16] For this step both sides of the second zinc porphyrin moiety are open for the ligand approach (Figure 1). The symmetrical approach, **a**, yields the *anti* species **1a·L**, which has two ligands orientated in opposite directions. This structure possesses a point chirality contribution to the CD signal due to

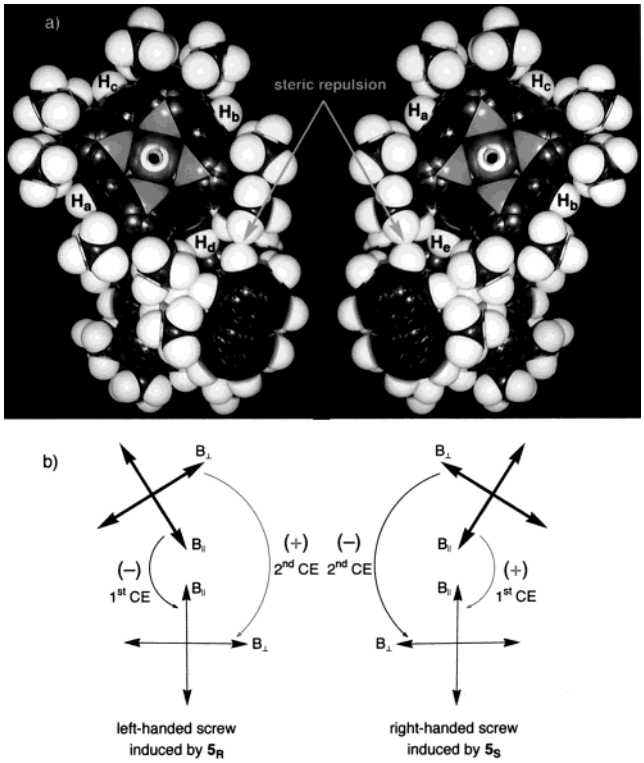

Figure 5. Mechanism of chirality induction in supramolecular systems **1·L** by chiral guests (where **L** = **5$_R$** and **5$_S$**): CPK models (a) and electronic transitions (b). The chiral ligand attached to the upper porphyrin ring is omitted for the clarity.

the direct ligand−zinc porphyrin interactions as described in the case of the monomeric host **15**. Although the conformational equilibria in **1a·L** may apparently exist due to a flexibility of the ethane bridge to give the whole range of the right-handed, left-handed, and non-screw structures, there are no visible driving forces such as steric hindrance, which can produce unidirectional structural deformations in this bis-porphyrin, and thus shift these equilibria to the particular direction, resulting in chirality induction in the whole supramolecular system. Alternatively, the asymmetrical approach, **b**, gives another atropisomer of the *anti* conformation **1b·L**, in which the chiral ligands are positioned on the same side of the porphyrin planes in the bis-porphyrin.[30] Additionally, **1b·L** may also be obtained by a ligand substitution process in **1a·L** via a ligand-exchange mechanism. This asymmetrical approach is apparently responsible for the process of supramolecular chirogenesis in **1**, because in **1b·L** there is a driving force for the total conformational equilibrium shift that, in turn, gives the stereospecific spatial arrangement of the coupling porphyrin chromophores in the resulted average structure of **1·L**.

The mechanism of the supramolecular chirogenesis is shown in Figure 5. When the second chiral ligand approaches from the same side of bis-porphyrin (approach **b**), it triggers a conformational turn of the neighboring ring in **1b·L**. Examina-

(30) A plausible explanation of the possible advantage for the asymmetrical approach **b** of the ligand to the bis-porphyrin **1** is as follows. Upon *syn* to *anti* conformational switching, the ethyl groups of the each porphyrin ring should be orientated in an opposite direction to reduce steric hindrances and thus to facilitate conformational switching. Apparently, the *syn* conformation of **1** has the same spatial arrangement of the ethyl groups to ensure strong intramolecular $\pi-\pi$ interactions between the porphyrin planes in **1**. As a consequence of this structural architecture, the asymmetrical approach **b** of the second ligand to the mono-ligated *anti* species formed after the first ligation should be sterically favorable, because the ethyl groups are directed outward and their rotation is relatively slow in the present conditions.[17]

tion of CPK molecular models reveals that there is a steric interaction between the X substituent of the chiral ligand and the ethyl group at either the 3- or 7-position of the neighboring porphyrin ring. The 3- or 7-position of the ethyl group adjacent to the ligand's X substituent is determined by the absolute configuration of the chiral guests. To reduce this steric repulsion a molecule of the bis-porphyrin adopts the corresponding screw conformation.[31] As this takes place, the corresponding pairs of the coupled $B_{||}$ and $B_{\perp}$ electronic transitions become optically active due to formation of the screw structure and thus exhibit exciton split CD signals. Although in the screw structure of **1b·L** there are no pure forbidden transitions and all eight possible transitions are in principle allowed, it is assumed that these two transitions are the major contributors to the observed Cotton effects as mentioned above. This assumption correlates well with the good match between the transitions observed in the UV−vis and CD spectra. However, on the basis of the data on the point chirality induction in the monomeric systems **15·L** due to the direct ligand−zinc porphyrin interactions (as discussed in section 2.2), this effect may have a small contribution (up to 11−17%) to the supramolecular chirogenesis in the bis-porphyrin systems **1·L**.

5. Role of the Guest's Absolute Configuration. As stated above, the steric interactions between the X substituent of the ligand and the ethyl groups of the neighboring porphyrin ring play a crucial role in the chiral structural deformation in the bis-porphyrin molecule **1b·L**. Therefore, the directions of the conformational twist should be dependent upon the absolute configuration of monoalkylamines studied. This is clearly demonstrated on CPK models of the systems **1b·5$_R$** and **1b·5$_S$** (Figure 5a). Thus, for the (*R*)-ligand **5$_R$**, steric repulsions between the naphthyl substituent and the ethyl group at the 7-position induce a left-handed screw, while the naphthyl group of the ligand **5$_S$** with *S* absolute configuration interacts with the ethyl group at the 3-position, producing a right-handed screw. This results in formation of the mirror images corresponding to the supramolecular structures **1b·5$_R$** and **1b·5$_S$**. Consequently, the optically active electronic transitions of these screw structures are mirror images as well, with the directions of the major coupling dipoles in **1b·5$_R$** and **1b·5$_S$** opposite to each other (Figure 5b). In particular, in a left-handed screw the coupling $B_{\perp}$ transitions produce a clockwise twist, while the coupling $B_{||}$ transitions give a counterclockwise twist. In the case of a right-handed screw, the coupling dipole directions are exactly opposite. According to CD exciton chirality theory[12] a clockwise orientation of two interacting electronic transitions produces positive chirality, while a counterclockwise orientation leads to negative chirality, and these orientations correspond to the positive and negative signs of the Cotton effects derived from the exciton coupling. If our assumption regarding the screw structure formation is right, it is expected that the first Cotton effect of **1b·L$_R$** with a left-handed screw, which is associated with the coupling $B_{||}$ transitions, will be negative, and the second Cotton effect related to the coupling $B_{\perp}$ transitions will be positive. Conversely, the supramolecular systems **1b·L$_S$** with a right-handed screw will produce opposite signs of the CD couplets. In practice, all of the chiral amines studied here, and alcohols studied previously,[6a] follow this rule showing negative chirality for the (*R*)-enantiomers and positive chirality for the (*S*)-enantiomers, regardless of the ligand structure (Table 2).

For the amines with several chiral centers (**6**, **7**, **9**) the signs of the Cotton effects are determined by the asymmetric carbon at the position that is closest to the coordinating amine group. For example, these are chiral carbons with (*S*) absolute configuration at the 2-position for **6$_S$** and **9$_S$**, and at the 3-position for **7$_S$**, exhibiting positive chirality (and negative chirality for the corresponding (*R*) absolute configuration at the 3-position for **7$_R$**). This is reasonable to expect, since the direction of the screw is based on the steric interactions between the X substituent and the ethyl group of the neighboring porphyrin ring, and hence the screw sense is determined by the asymmetric carbon that is the closest to this interaction site.

The ^{1}H NMR spectra of the right- and left-handed screw structures, as would be expected for mirror images, must be identical, since static ^{1}H NMR spectroscopy is not sensitive to the screw direction. However, the ^{1}H NMR signals of the right- and left-handed screws with the same chemical shift are indeed derived from the different proton resonances that were shown by the ^{1}H NMR dynamic experiments.[32] The reason is that the spatial location of the same proton in relation to the neighboring porphyrin ring is different for the right- and left-handed screws, resulting in different proton exposure to the ring current effect (for example, H_a, H_b and H_d, H_e pairs, see Figure 5a). On the other hand, the H_a resonance of the left-handed screw and the H_b resonance of the right-handed screw are at the same location in relation to the neighboring porphyrin ring, and hence affected by its ring current effect to the same extent. This is clearly demonstrated with **1·4$_R$** and **1·4$_S$** (see Figure 4c,d). The singlet of the *meso* protons of **1·4$_R$** at 10.01 ppm arises from the H_a resonance, while the same singlet of **1·4$_S$** is due to the H_b resonance. In the case of the singlet at 9.96 ppm, the situation is directly opposite. The same tendency of the proton peak interconversion is observed for the $-CH_2CH_2-$ bridge protons (H_d and H_e) and $-C\underline{H}_2CH_3$ protons. However, the *meso* H_c resonance is not affected by the inversion process. This is due to the spatial location of H_c, which is the same in relation to the neighboring porphyrin ring in both screw structures, and thus H_c has the same exposure to the ring current effect.

6. Role of the Guest's Bulkiness at the Chiral Center. Considering steric repulsions as the major driving forces for the screw formation resulting in the supramolecular chirogenesis as discussed above, it is obvious that the size of the X substituent is of prime importance for these steric interactions, and hence should be an influential factor controlling the process of asymmetry transfer. This suggestion is fully supported by the CD and ^{1}H NMR experimental data obtained for the supramolecular systems **1·2**−**1·7**, **1·10**, and **1·11**. In general, amines with the bulkier X substituents induce Cotton effects of greater intensity (Table 2, Figure 3a−c), while the positions of the CD (as well as UV−vis) signals remain essentially unchanged. This is demonstrated most clearly on an example of the type A amines, which are structural homologues. In particular, it was found that the total CD signal amplitude ($|A|$ which is determined according to footnote c of Table 2) is linearly dependent on the effective size of amine, which is a special bulkiness parameter (Figure 6). Since the two porphyrin planes are in a parallel orientation in **1·L**, the strongest steric interactions between the X substituent on the asymmetric carbon of the chiral amine and the ethyl group of the neighboring porphyrin ring are expected to be in the plane parallel to the porphyrin ring, which is supported by CPK model analysis. Therefore, the effective size was determined as follows (Chart 1). The N−C* bond of the MM2-optimized amine was placed perpendicular to the projection plane (bold line). The effective

(31) Although there is a possibility of formation of the whole range of differently orientated *anti* conformations, the screw conformation is the least sterically hindered and thus the most probable structure.

(32) Borovkov, V. V.; Lintuluoto, J. M.; Inoue, Y. *J. Phys. Chem. A* **2000**, *104*, 9213−9219.

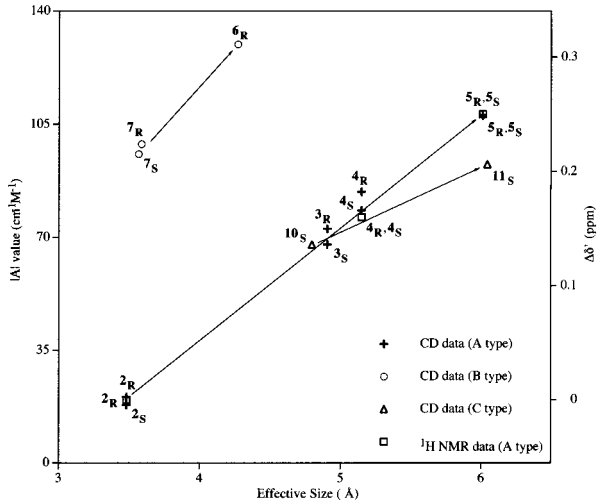

Figure 6. Dependence of the value of the CD total amplitude ($|A|$) and chemical shift difference ($\Delta\delta'$) of the A, B, and C homologous types of the ligands on the effective size of the amines (see Chart 1). The homologous type of the ligands is shown by the same symbols and arrows.

size (in Å) is the horizontal distance between the N atom and the most distant atom of the X substituent. It is important to note that the simple length or volume of the X substituent, or the whole amine molecule as a bulkiness parameter, does not give any clear correlation with the $|A|$ values.

It should be noted also that for two other structurally homologous series of the ligands (types B and C) the same tendency is observed (Figure 6). The systems **1·6$_R$** and **1·11$_S$** with bulkier amines, and hence greater effective sizes, result in larger $|A|$ values in comparison to corresponding analogues **1·7$_{R,S}$** and **1·10$_S$** with smaller effective sizes, although the number of experimental points is not sufficient to obtain dependencies as in the case of the homologous type A.

The effect of the ligand bulkiness is clearly seen in the ^{1}H NMR spectra of the supramolecular systems **1·L** for the type A of the amine's structural homologues as well (Table 3, Figure 4). The spectral profile of the less bulky **1·2$_R$** (Figure 4b) is almost the same as that of **1·L**, where **L** are achiral alcohols[16] or racemic amines.[6a] In contrast, systems **1·4** and **1·5** containing bulkier aromatic amines exhibit remarkably different ^{1}H NMR pattern. In particular, the 10,20-*meso* protons and $-CH_2CH_2-$ bridge protons are split into two signals of equal intensity (H_a, H_b and H_d, H_e pairs, respectively, see Figure 4c−e). The differences in chemical shift ($\Delta\delta'$) between H_a, H_b and between H_d, H_e peaks are 0.05−0.10 ppm and 0.16−0.25 ppm, respectively. Also the $-C\underline{H}_2CH_3$ protons of **1·4** and **1·5** are better resolved in comparison to those of **1·2**. Thus, there are four (for **1·4$_R$** and **1·4$_S$**) or five (for **1·5$_R$**) multiplets including resolved quadruplets in the upfield (for **1·4** and **1·5**) and downfield (for **1·5**) regions, while there are only two broad multiplets in the case of **1·2$_R$**.

Interestingly, the $\Delta\delta'$ values of the $-CH_2CH_2-$ bridge protons[33] when plotted versus the amine effective size coincide perfectly with the $|A|$ values obtained from the CD data, and exhibit identical linear dependence (Figure 6). This result indicates that the spectral changes monitored by different spectroscopic methods are actually a result of the same structural deformations in **1** induced by the bulkier X substituents. Furthermore, this good matching of the CD and ^{1}H NMR dependencies support unambiguously the mechanism of supramolecular chirality induction via screw formation as a result of steric interactions.

Chart 1

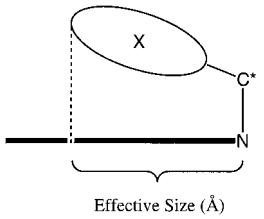

The role of the ligand bulkiness in the chirogenesis process can be easily understood by analyzing CPK molecular models. Thus, a comparison of the models of **1·4$_R$** and **1·5$_R$** reveals that the bulkier naphthyl group (in the case of **1·5$_R$**) produces a stronger steric repulsion and consequently a greater screw in the averaged *anti* conformation of **1·L**[34] in order to minimize steric hindrances (Figure 7a). It is obvious, that the change of the degree of the interporphyrin screw affects spatial orientation of the interacting porphyrin transitions (Figure 7b). The dihedral angle between the $B_{||}$ dipoles of **1·5$_R$** (α) becomes smaller than that of **1·4$_R$** (α'), while the angle between the corresponding $B_\perp$ dipoles becomes larger (β of **1·5$_R$** > β' of **1·4$_R$**).

Although reliable theoretical treatment of optical activity in bis-porphyrins is not available yet, numerical calculations of the CD spectra of simple bis-benzoates using the exciton chirality method[12] showed that the amplitude of Cotton effects has a parabolic-like dependence on the dihedral angle between the coupling transitions, with zero values at 0° and 180° and a maximum value at around 70°. This dependence is schematically shown in Figure 7c. Assuming that in general the coupling dipoles follow this tendency, our experimental results can be empirically rationalized as follows. Upon increasing the degree of screw, the angle between $B_\perp$ dipoles becomes larger moving from the β' value to the β value and following the curve from 0° to the maximum, while the angle between the $B_{||}$ dipoles becomes concurrently smaller moving from the α' value to the α value and following the curve from 180° to the maximum. These angle changes result in overall increase of the total CD amplitude ($A > A'$).

The change in the screw degree is also the reason for the dependence of the $\Delta\delta'$ values on the amine effective size. Indeed, in the case of the greater left-handed screw induced in **1·5$_R$** the H_a, H_b and H_d, H_e protons become less equivalent in comparison to the corresponding proton pairs of the lesser screw induced in **1·4$_R$** (Figure 7a). This is due to different exposure of these protons to the ring current effect of the neighboring porphyrin ring. Owing to this, the largest splitting between the H_a, H_b and H_d, H_e resonances is expected for the less symmetrical structure **1·5$_R$**, and indeed, this is experimentally observed (Table 3, Figure 4).

7. Role of the Guest's Bulkiness at the Amino Binding Site. Since the guest bulkiness at the chiral center plays a key role in controlling supramolecular chirogenesis as shown above, it is essential to investigate other bulkiness factors which can also directly affect this chirality induction process. Among these factors, the steric hindrance variation at the amino binding group

(33) The $-CH_2CH_2-$ bridge protons are chosen as monitoring parameters because the positions of their resonances are the least affected by the background *syn*−*anti* conformational changes.[6a,16]

(34) This average conformation is a result of the overall equilibrium between the right-handed, left-handed, and non-screw linear structures in **1·L**. Existence of this equilibrium is proved by comparison of the anisotropy factor ($g = \Delta\epsilon/\epsilon$) for the supramolecular systems **1·L** at low temperatures[6a] and at room temperature. The g factors, which are presumably independent of the concentration change upon lowering the temperature, are found to be in 2−4 times larger at low temperatures.

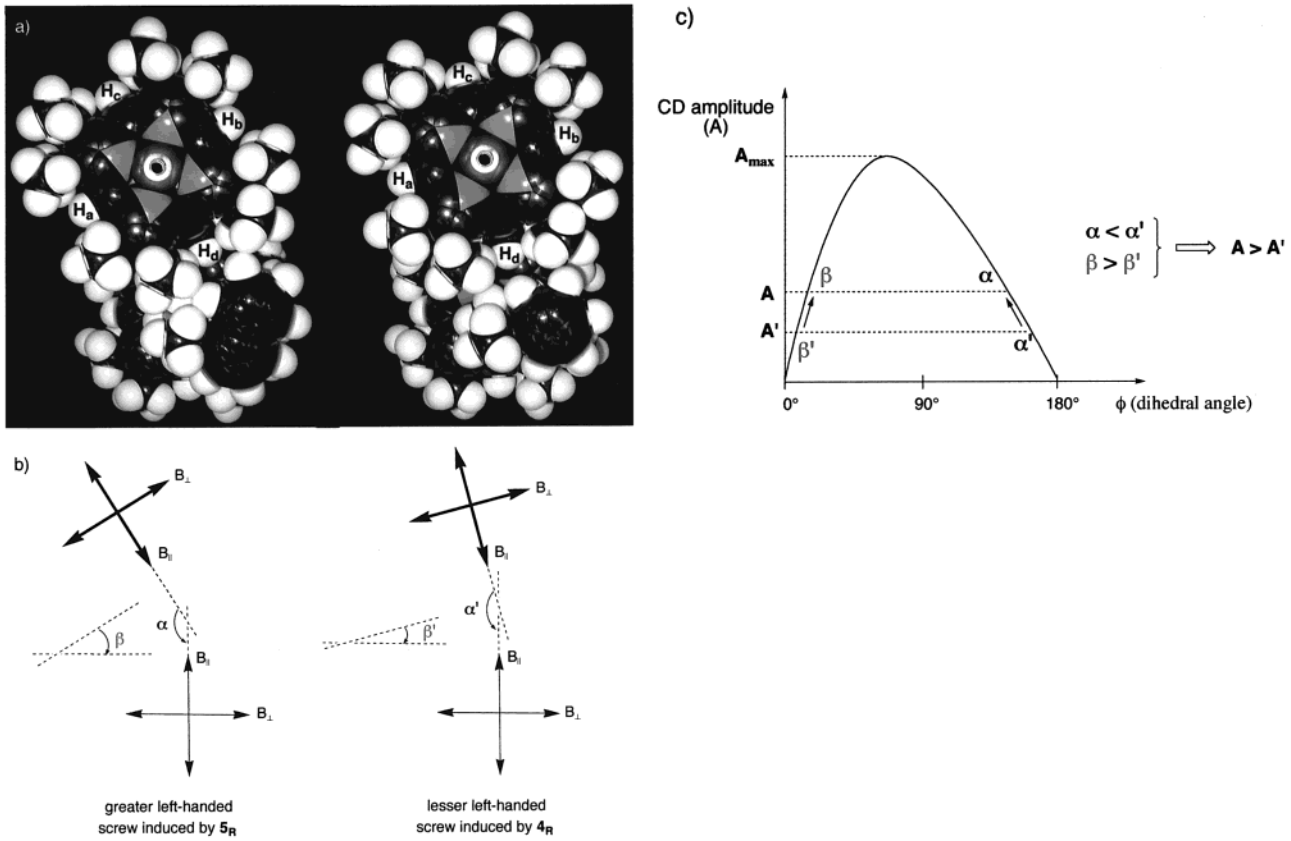

Figure 7. The size effect of the chiral guest on the supramolecular chirality induction in **1·L** (where $\mathbf{L} = \mathbf{5_R}$ and $\mathbf{4_R}$): CPK models (a), electronic transitions (b), and schematic representation of the CD amplitude dependence on the dihedral angles (ϕ) between the corresponding electronic transitions (c).

by simple N-substitution effect is another important element which should be considered.

To investigate this influence, type E chiral amines were used to induce chirality in **1·L**. Upon increasing the bulkiness around the binding site by subsequent substitution of the free amino group of **4** at first with a methyl group (in the case of **13**) and then with a benzyl group (in the case of **14**), the total CD amplitude is changed as shown in Figure 8. The amine achiral substituent size was chosen as the parameter of the amino group bulkiness and was determined as the distance between the N atom and the most distant H atom of the corresponding N-substituent (R) at the amino group of the MM2-optimized amine structure (Chart 2). The initial step of bulkiness increase by moving from the N-unsubstituted ligand **4** to methylated **13** results in noticeable enhancement of the $|A|$ value, while further increase of the R substituent size by introduction of the benzyl group (in the case of **14**) leads to a considerable decrease of the CD amplitude (Table 2, Figure 8). This behavior is unusual at first sight, since the binding constants of zinc porphyrins with secondary amines are smaller than those with primary amines.[19,35] Therefore, it might be expected that the $|A|$ value of methylated **13** should also decrease in comparison to that of unsubstituted **4**. However, the binding factor can be neglected in this case because saturated amine concentrations (see footnote a of Table 2) are used in this study, hence shifting the overall equilibria to the fully bound structures whose formation was monitored by UV−vis spectroscopy. Therefore, this dependence of the $|A|$ value should be mostly considered from a steric point of view and can be easily understood by analyzing CPK molecular models. This analysis reveals that the methyl group of **13** is small enough not to prevent facile access of the amino group to the zinc ion during asymmetrical approach **b** (Figure 1) to form the chiral supramolecular structure **1b·L**. On the other hand, the additional bulkiness around the amino binding site results in a chirality enhancing effect, fixing the neighboring porphyrin ring more tightly in a particular screw handedness (left-handed for (*S*)-ligands and right-handed for (*R*)-ligands),

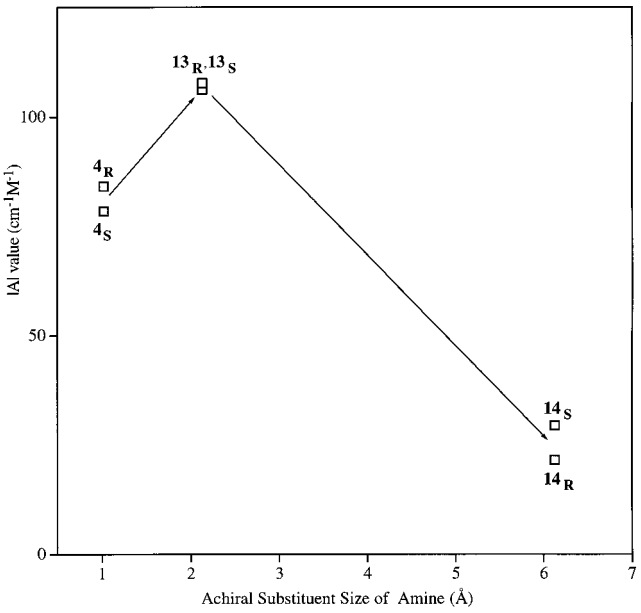

Figure 8. Dependence of the value of the CD total amplitude ($|A|$) of the E homologous type ligands on the amine achiral substituent size (see Chart 2).

(35) ΔG_{293}(kcal·mol^{-1}) = −6.7 for $\mathbf{1{\cdot}4_{R,S}}$ and −5.6 for $\mathbf{1{\cdot}13_{R,S}}$.

Chart 2

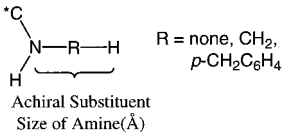

hence shifting the overall equilibrium of the screw structures unidirectionally. This subsequently results in enhancement of the CD amplitude. In the case of the benzyl derivative **14**, the amino group becomes too bulky, making its access to the zinc ion more sterically hindered from the asymmetrical side **b**. This leads to formation of the *anti* species from the symmetrical approach **a** increasing the population of the corresponding conformer **1a·L**, which is not supramolecularly optically active as discussed above. These results show clearly the importance of the binding site bulkiness in controlling supramolecular chirality induction process.

8. Role of the Chiral Center Position. Besides bulkiness, another important question regarding supramolecular chirogenesis is a sensitivity of the host molecule **1** with respect to the proximity of the guest's chiral center, in other words, whether chiral induction in **1** is possible due to preferential screw formation upon complexation of the ligands with the asymmetric carbon moved away from the binding site. To answer this question, the amines **8**, **9**, and **12** (type D) were used to study the chirogenesis process in **1**. Although, as expected, the CD intensities of these systems are greatly reduced (more than 1.5 times) in comparison to those of the corresponding structural analogues **2** and **10**, the chirality sign remains intact, showing the positive sign for the (*S*) absolute configuration (**1·8**$_S$, **1·9**$_S$, **1·12**$_S$) and the negative sign for the (*R*) absolute configuration (**1·12**$_R$) (see Table 2). It is assumed that the mechanism of chirality induction in **1** by these amines is essentially the same as for the all other ligands studied. The only difference is that, upon moving the chiral carbon away from the binding amino site, the steric interactions between the ligand and the neighboring porphyrin ring are considerably reduced, thus decreasing the probability of formation of the corresponding unidirectional screw, due to an inadequate equilibrium shift between the right-handed and left-handed screw structures and leading to substantial reduction of the induced CD signals.

Nevertheless, these data demonstrate undoubtedly a high chiroptical sensitivity of the host molecule **1** to the external guest molecules with a distant chiral center. This makes it possible to differentiate even a very low level of asymmetry, such as methyl and ethyl substituents at the asymmetric carbon located at the β-position with respect to the binding site.

9. Application for the Absolute Configuration Determination. As discussed above the chirality sign is dependent upon the ligand's absolute configuration, with positive chirality observed for the (*S*)-enantiomers of the amines studied here and of the alcohols studied previously,[6a] and negative chirality observed for the corresponding (*R*)-enantiomers (Table 2). This sign, according to the postulated mechanism, is governed by the screw direction, which depends on the order of the substituent's bulkiness at the asymmetric carbon. Therefore, in the cases when the absolute configuration is determined by the size of the substituents, host molecule **1** can be successfully applied for determination of the guest's absolute configuration. In particular, this method is best suited for various monoamines, alcohols, and other compounds with different mono functional groups, which are able to coordinate to bis-metalloporphyrins.

This method can be also applied for compounds with several chiral centers. Thus, in the case of guest molecules containing two or more chiral centers the CD sign reflects the absolute configuration of the asymmetric carbon which is the closest to the binding site. For example, **1·6**$_S$, **1·7**$_S$, and **1·9**$_S$ exhibit positive chirality, while **1·7**$_R$ shows negative chirality. This selectivity is due to the same mechanism of directional screw formation, which was discussed above for the systems with a single chiral center.

The obvious merits of this supramolecular system are a high sensitivity and noncovalent character of the interaction, allowing full recovery of all components after their use. Furthermore, an additional advantage of this method is in situ use of chiral ligands without their chemical derivatization.

Conclusions

This work clearly demonstrates that the chiral guest structure plays an important role in supramolecular chirality induction by controlling the conformational changes in the achiral host molecule via a steric repulsion mechanism resulting in selective screw formation. In particular, induced chirality is dependent upon the ligand's bulkiness and absolute configuration. These results offer a clearer view of supramolecular chirogenesis in natural and artificial systems and may have practical implications in the design of chiroptical molecular devices. Specifically, a high chiroptical sensitivity of the host molecule to external guest molecules makes it possible to use this system for determining the absolute configuration of chiral compounds even when the asymmetry at the chiral center is low. Further studies to enhance the applicability and sensitivity of this system to other types of chiral compounds are currently in progress and will be the subject of future reports from our group. Finally, the realization and application of this general methodology to other supramolecular systems should provide a powerful and versatile technique for the elucidation of the detailed mechanisms of chirality induction in both artificial and natural assemblies.

Acknowledgment. We thank Dr. G. A. Hembury for assistance in the preparation of this manuscript.

JA0032982